

# Supplemental Information

This Supplemental Information for “GCAM-CDR 1.0: Enhancing the Representation of Carbon Dioxide Removal in an Integrated Assessment Model” covers technical details of the new CDR technologies included in GCAM-CDR 1.0. Variants on these technologies, using different parameters and/or different inputs, can be added to the model fairly easily.

## A Note on Implementation of Negative Emissions in GCAM-CDR

Like GCAM 5.4, GCAM-CDR calculates positive and negative emissions by tracking the carbon content of each technology’s inputs and outputs. If the outputs of a technology (e.g., electricity) contain less carbon than its inputs (e.g., coal), then the difference is reported as emitted carbon, unless that carbon is captured and sequestered. If the outputs of a technology contain more carbon than its inputs, however, the difference is reported as negative emissions. In GCAM-CDR, all of the newly introduced CDR technologies consume an abstract input called “atmospheric CO<sub>2</sub>” in the regional CDR sector, downstream from the technologies described below. The “atmospheric CO<sub>2</sub>” input has a carbon coefficient of –1, and the output (“CDR\_regional”) has a carbon coefficient of 0, so that the model perceives the technology as creating negative emissions. This approach differs slightly from the one used in GCAM 5.4 to model negative emissions in its DAC technologies.

## Technology Descriptions

### Direct Air Capture

GCAM-CDR includes two kinds of DAC, as described in Sect. 2.3.1 and 2.3.2 of the main text. Both are parameterized based on work by Realmonte et al. (2019), which is consistent with other published literature on these technologies.

Note that because the negative emissions for all new CDR technologies in GCAM-CDR are modeled downstream, in the regional CDR sector, both DAC technologies consume a placeholder good (labeled “solvent” or “sorbent” but not reflecting any meaningful properties of those inputs in the real world) with a carbon coefficient of 1. Because that carbon is immediately sequestered, the model does not count it as emitted carbon or a negative emission. It is included to force the DAC technologies to internalize the endogenously calculated cost of carbon sequestration and to accurately track the amount of carbon that DAC technologies inject into geological reservoirs.

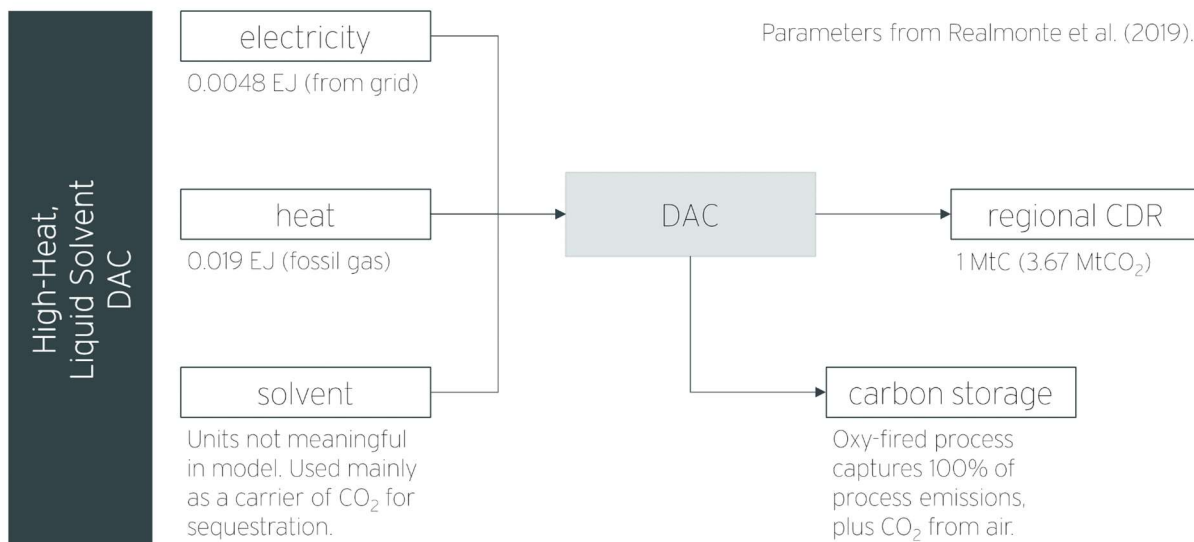


**Figure S1. A diagram of the high-heat, liquid solvent-based DAC technology included in GCAM-CDR 1.0.**

30

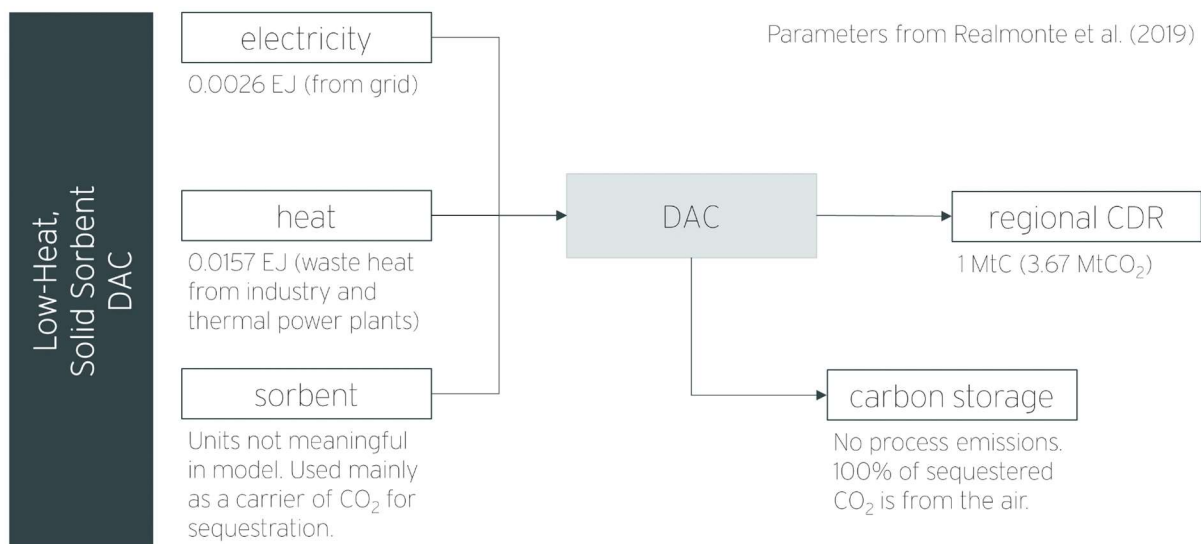


**Figure S2. A diagram of the low-heat, solid sorbent-based DAC technology included in GCAM-CDR 1.0.**

## Terrestrial Enhanced Weathering

GCAM-CDR 1.0 includes one approach to terrestrial enhanced weathering (basalt application to cropland), as described in Sect. 2.3.3 of the main text. Parameters are based on work by Streffler et al. (2018).

Note that the “cropland” input (called “cropland\_TEW” in model input files) is an abstract, finite, renewable resource that represents cropland available for basalt application. The maximum quantity available in a region is exogenously specified based on GCAM’s reported cropland in each region in 2020. An upward-sloping supply curve for the resource represents the assumption that basalt will be applied to the most easily accessible croplands first, with additional application becoming increasingly more expensive because of the need to transport basalt to more distant or inaccessible areas.

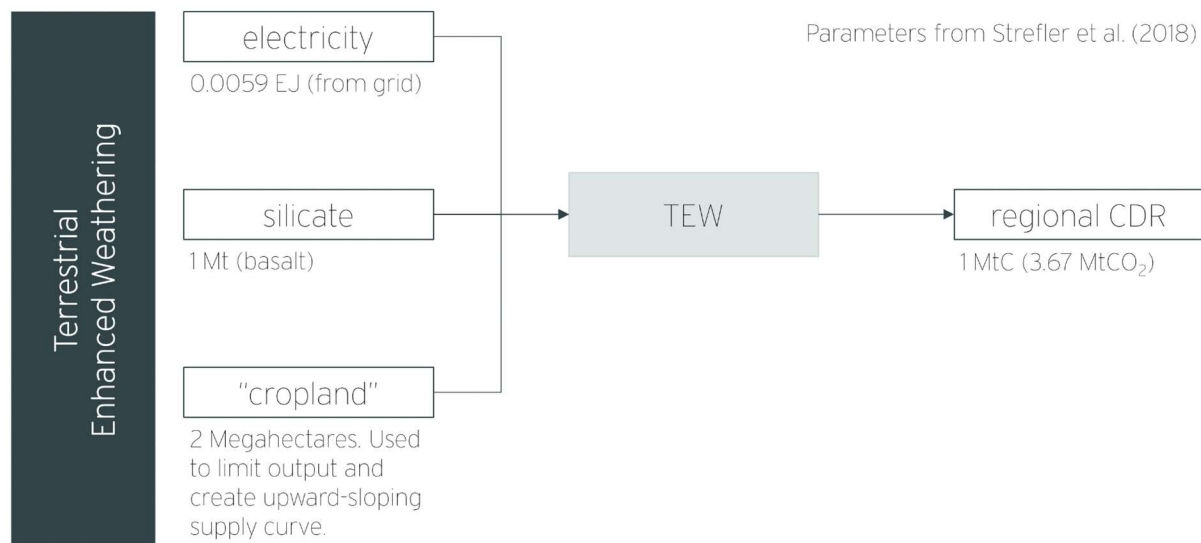


**Figure S3. A diagram of the terrestrial enhanced weathering (TEW) technology included in GCAM-CDR 1.0.**

## Ocean Enhanced Weathering

GCAM-CDR includes one technology for ocean-based enhanced weathering (ocean liming), as described in Sect. 2.3.4 of the main text. Parameters for this technology are based mainly on the oxy-flash calcination process described by Renforth et al. (2013). This approach to lime production captures the process emissions from both combustion of natural gas and calcination of limestone simultaneously.

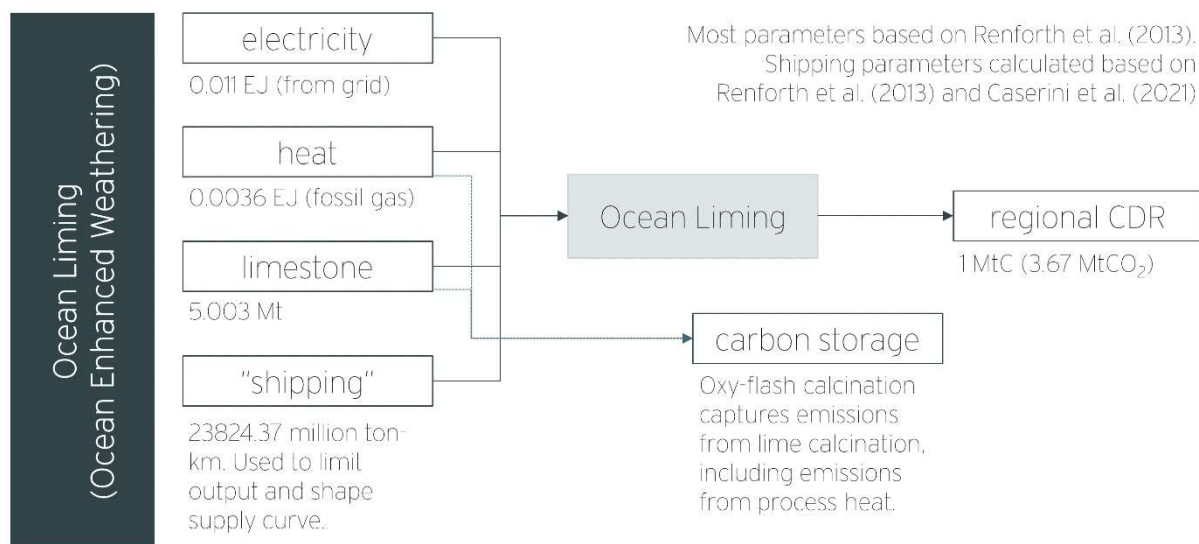


**Figure S4. A diagram of the ocean liming technology included in GCAM-CDR 1.0.**

GCAM-CDR 1.0 assumes that ocean liming is conducted using cargo ships, rather than a dedicated fleet of ocean liming vessels, and that this creates a potentially binding constraint on global capacity for ocean liming. To capture this constraint, we model ocean liming as requiring an abstract good, “OEW-shipping,” that is produced as a byproduct of international maritime freight. GCAM measures maritime freight in million ton-kilometers and calculates the price per ton-km. The key exogenous parameters, for our purposes, are the number of ton-kms per ton of CDR and the maximum percentage of maritime freight that could be devoted to OEW.

We calculate the first parameter in two independent ways: bottom-up, using estimates from Renforth et al. (2013), and top-down, using estimates from Caserini et al. (2021). Caserini et al. estimate that bulk and container cargo ships could devote 13% of their tonnage to OEW, and that if all bulk and container cargo ships did so, they could deliver 1,700–4,000 Mt of lime into the ocean each year, depending on whether they stop to load more lime mid-route. Bulk and container cargo ships provide approximately 72% of maritime freight by ton-km (UN Conference on Trade and Development, 2020), implying that it would take approximately 9.36% of total global maritime freight capacity to release 1,700 Mt of lime into the ocean each year. GCAM estimates global shipping volume at 119,203,204 million ton-km annually in 2020, implying a rate of 6,563 million ton-km per Mt of lime released. At a rate of 3.63 Mt of slaked lime per MtC removed—as calculated by Renforth et al. (2013)—this implies a coefficient of 23,824.37 million ton-km per MtC removed. This is within 2% of our bottom-up estimate calculated based on parameters from Renforth et al. (2013). Strictly speaking, this is an overestimate of the number of ton-kms that would be needed, as the tonnage of slaked lime that needs to be moved would decline linearly during transit

as it is dumped into the sea. As the purpose of this model input is to capture the way in which shipping *capacity* acts as a constraint on ocean liming, rather than just an additional cost to be born, we ignore this complication.

The second key parameter is the total fraction of maritime shipping that could be devoted to OEW. Here we follow Caserini et al. (2021) and impose an upper limit of 13%, but in interpreting this number, it is important to note two things.

75 First, Caserini et al. (2021) assume that ships carry both lime and other cargo. Second, many cargo ships, especially bulk cargo ships, frequently sail empty because the countries that export bulk cargo, such as iron ore or wheat, tend not to import bulk cargo (Brancaccio et al., 2017). Thus, this number does not imply that 13% of other maritime freight would have been displaced. The estimates from Caserini et al. (2021) align reasonably well with earlier estimates from Köhler et al. (2013) that global shipping capacity in 2007 was sufficient to deliver approximately 10 Gt of material into the ocean.

80 Another important implication of the frequent mismatch because cargo ships and available cargo is carriers often ship goods at steep discounts on routes where they would otherwise sail empty (Brancaccio et al. 2017). To capture this, we assume that the costs of shipping for ocean liming begin well below the endogenously calculated cost of maritime freight, but rise to parity with shipping of other freight as ocean liming approaches the limit of 13% of global capacity.

Finally, note that because we model the OEW-shipping placeholder good as a by-product of maritime freight, the  
85 value of that good lowers the net cost of maritime freight. In GCAM, this induces a slight increase in maritime freight, so that the growth of ocean liming causes some growth in total maritime shipping.

## References

Brancaccio, G., Kalouptsi, M., and Papageorgiou, T.: Geography, Search Frictions and Endogenous Trade Costs, National Bureau of Economic Research, Cambridge, MA, <https://doi.org/10.3386/w23581>, 2017.

90 Caserini, S., Pagano, D., Campo, F., Abbà, A., De Marco, S., Righi, D., Renforth, P., and Grosso, M.: Potential of Maritime Transport for Ocean Liming and Atmospheric CO<sub>2</sub> Removal, 3, 2021.

Köhler, P., Abrams, J. F., Völker, C., Hauck, J., and Wolf-Gladrow, D. A.: Geoengineering impact of open ocean dissolution of olivine on atmospheric CO<sub>2</sub>, surface ocean pH and marine biology, *Environ. Res. Lett.*, 8, 014009, <https://doi.org/10.1088/1748-9326/8/1/014009>, 2013.

95 Realmonte, G., Drouet, L., Gambhir, A., Glynn, J., Hawkes, A., Köberle, A. C., and Tavoni, M.: An inter-model assessment of the role of direct air capture in deep mitigation pathways, 10, 1–12, <https://doi.org/10.1038/s41467-019-10842-5>, 2019.

Renforth, P., Jenkins, B. G., and Kruger, T.: Engineering challenges of ocean liming, *Energy*, 60, 442–452, <https://doi.org/10.1016/j.energy.2013.08.006>, 2013.

100 Strefler, J., Amann, T., Bauer, N., Kriegler, E., and Hartmann, J.: Potential and costs of carbon dioxide removal by enhanced weathering of rocks, *Environ. Res. Lett.*, 13, 034010, <https://doi.org/10.1088/1748-9326/aaa9c4>, 2018.

UN Conference on Trade and Development: UNCTAD Handbook of Statistics, United Nations Publications, New York, 2020.